

B_s mesons: semileptonic and nonleptonic decays

C. Albertus^{1,a}, E. Hernández², C. Hidalgo-Duque³, and J. Nieves³

¹Departamento de Física Atómica, Nuclear y Molecular e Instituto Carlos I de Física Teórica y Computacional, Universidad de Granada, Avenida de Fuentenueva s/n, E-18071 Granada, Spain

²Departamento de Física Fundamental e IUFFyM, Universidad de Salamanca, Plaza de la Merced s/n, E-37008 Salamanca, Spain

³Instituto de Física Corpuscular (IFIC), Centro Mixto CSIC -Universidad de Valencia, Institutos de Investigación de Paterna, Apartado 22085, E-46071 Valencia, Spain

Abstract. In this contribution we compute some nonleptonic and semileptonic decay widths of B_s mesons, working in the context of constituent quark models [1, 2]. For the case of semileptonic decays we consider reactions leading to kaons or different $J^P D_s$ mesons. The study of nonleptonic decays has been done in the factorisation approximation and includes the final states enclosed in Table 2.

1 Introduction

The description of CP violation in the Standard Model demands an accurate knowledge of the Cabibbo-Kobayashi-Maskawa (CKM) quark mixing matrix. Being the b-sector the one known with lesser precision, a precise quantitative study of the weak decays of B and B_s mesons is needed. In this contribution we summarise our studies of the semileptonic decays B_s into K and D_s states, and some of the nonleptonic decays studied in Refs.[1, 2], evaluated in the context of a constituent quark model.

2 Semileptonic $B_s \rightarrow K$ decay

The hadronic matrix element for this decay can be parametrised in terms of the form factors f_+ and f_0 . If we neglect the mass of the leptons, only f_+ contributes to the differential decay width

$$\frac{d\Gamma}{dq^2} = \frac{G_F^2}{192\pi^3} |V_{ub}|^2 \frac{\lambda^{3/2}(q^2, M_{B_s}^2, M_K^2)}{M_{B_s}^3} f_+^2(q^2) \quad (1)$$

with G_F being the Fermi constant, $|V_{ub}|$ the modulus of the corresponding CKM matrix element and $\lambda(a, b, c) = a^2 + b^2 + c^2 - 2ab - 2ac - 2bc$.

We evaluate the valence quark contribution to the form factor that we supplement with a B^* -pole one to improve its behaviour at high q^2 values [1]. To extend the above predictions beyond its region of applicability (near q_{\max}^2), we adopt a multiply-subtracted Omnes dispersion relation [3–6], and we take

$$f_+(q^2) \approx \frac{1}{M_{B^*}^2 - q^2} \prod_{j=0}^n [f_+(q_j^2)(M_{B^*}^2 - q_j^2)]^{\alpha_j(q^2)}, \quad \alpha_j(q^2) = \prod_{j \neq k=0}^n \frac{q^2 - q_k^2}{q_j^2 - q_k^2} \quad (2)$$

^ae-mail: albertus@ugr.es

Table 1. Branching fractions for the indicated decay channels, in percentage.

M'	$l = e, \mu$	$l = \tau$
D_s^+	2.32	0.67
D_{s0}^{*+}	0.39	0.04
D_s^{*+}	6.26	1.53
$D_{s1}^+(2460)$	0.47	0.04
$D_{s1}^+(2536)$	0.32	0.03
$c\bar{s}(2^-)$	$9.2 \cdot 10^{-3}$	$2.0 \cdot 10^{-4}$
D_{s2}^{*+}	0.44	0.03

for $q^2 < s_{th} = (m_{B_s} + m_K)^2$ and where the different $q_j^2 \in]-\infty, s_{th}[$ are the different subtraction points. The values of the f_+ form factor at the subtraction points are taken as free parameters that we fit to our quark model results (valence plus B^* -pole) at high q^2 and previous light cone sum rules (LCSR) results in the low q^2 region [7]. We take the subtraction points at $q^2 = 0, q^2 = \frac{q_{\max}^2}{3}, q^2 = \frac{2q_{\max}^2}{3}$ and $q^2 = q_{\max}^2$. In the left panel of Fig. 1 we compare the f_+ form factor obtained in our combined

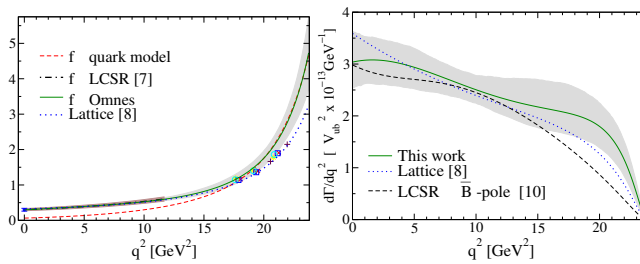


Figure 1. Left panel: Comparison of the different approaches to the f_+ form factor. Right panel: Differential decay width calculated with a 68% confidence level band obtained with our fitting procedure.

approach with the ones calculated using LCSR techniques [7] and lattice QCD [8]. The latter are an extrapolation of the lattice points obtained in Ref. [9] which are also shown. In the right panel, we plot the differential decay width. We compare our results with the ones in Ref. [10], obtained in a LCSR+ B^* -pole calculation, and in Ref. [8], obtained in lattice QCD. In both panels we also include a 68% confidence level band for our predictions. The total decay width that we get is $\Gamma(B_s \rightarrow Kl^+\nu_l) = (5.47^{+0.54}_{-0.46})|V_{ub}|^2 \times 10^{-9}$ MeV. This is to be compared with the results $(4.63^{+0.97}_{-0.88})|V_{ub}|^2 \times 10^{-9}$ MeV [10], where we have propagated a 10% uncertainty in the form factor, and $(5.1 \pm 1.0)|V_{ub}|^2 \times 10^{-9}$ MeV [8]. The three estimates are compatible within uncertainties. More details are given in Ref. [1].

3 Semileptonic $B_s \rightarrow D_s^{(*)}$ decays

We have considered the semileptonic decays of B_s meson into $D_s^{(*)}$ states with J^π quantum numbers $0^-, 0^+, 1^-, 1^+, 2^-$ and 2^+ . The form factor decomposition required for each channel can be found in Ref. [2]. We have adopted the helicity formalism of Ref. [11] to compute the contraction of the leptonic and hadronic tensors. Expressions for the helicity amplitudes can be found in Ref. [2].

In Table 1 we show our results for the branching ratios. As shown in Table V of Ref. [2] the results of this work are in good agreement with those from Ref. [12], obtained in a relativistic quark model

approach. The agreement is also good with the quark model calculation of Ref. [13]. Our results for decays into orbitally excited final D_s^* mesons agree with our previous results from Ref. [14], though in that work the potential model that has been used was much more sophisticated. Our results also compare well to the sum-rules calculation of Refs. [15, 16], while the result of Ref. [17] is lower by a factor of two. The same happens if we compare with the results of Ref. [18] or Ref. [19]. In Ref. [2] we also check our results against Heavy Quark Symmetry predictions.

4 $\bar{B}_s \rightarrow c\bar{s}M_F$

We have also calculated the decay width for two-meson nonleptonic reactions $\bar{B}_s \rightarrow c\bar{s}M_F$ where M_F is a light pseudoscalar or vector meson. These decays correspond to a $b \rightarrow c$ transition at the quark level. These transitions are governed, neglecting penguin operators, by the effective Hamiltonian of Eq. (53) of Ref [2]. See Refs. [20, 21] for further details. We shall work in the factorisation approximation, i. e., the hadron matrix elements of the effective Hamiltonian are evaluated as a product of quark-current matrix elements. One of these is the matrix element of the B_s transition to one of the final mesons, while the other is determined by the decay constant of the other meson. In Table 2 we compare our calculations with previous results and experimental data when available. More results are shown in Ref. [2].

Acknowledgements

This research was supported by the Spanish Ministerio de Economía y Competitividad and European FEDER funds under Contracts Nos. FPA2010-21750-C 02-02, FIS2011-28853-C02-02, and CS D2007-00042, by Generalitat Valenciana under Contract No. PROMETEO/20090090, by Junta de Andalucía under Contract No. FQM-225, by the EU HadronPhysics3 project, Grant Agreement No. 283286, and by the University of Granada start-up Project for Young Researchers contract No. PYR-2014-1. C.A. wishes to acknowledge a CPAN postdoctoral contract and C.H. -D. thanks the support of the JAE-CSIC Program.

References

- [1] C. Albertus, E. Hernández, C. Hidalgo-Duque, J. Nieves, Phys. Lett. B **738**, 144 (2014).
- [2] C. Albertus, Phys. Rev. D **89**, 065042 (2014).
- [3] C. Albertus, J. Flynn, E. Hernandez, J. Nieves, J. Verde-Velasco, AIP Conf. Proc. **892**, 312 (2007).
- [4] J.M. Flynn, J. Nieves, Phys. Rev. D **76**, 031302 (2007).
- [5] J.M. Flynn, J. Nieves, Phys. Lett. B **649**, 269 (2007).
- [6] J.M. Flynn, J. Nieves, Phys. Rev. D **75**, 013008 (2007)
- [7] G. Duplancic, B. Melic, Phys. Rev. D **78**, 054015 (2008)
- [8] C. Bouchard, G.P. Lepage, C. Monahan, H. Na, J. Shigemitsu, Phys. Rev D **90**, 054506 (2014).
- [9] C. Bouchard, G.P. Lepage, C.J. Monahan, H. Na, J. Shigemitsu (2013), arXiv:1310.3207 [hep-lat] (2013).
- [10] Z.H. Li, F.Y. Liang, X.Y. Wu, T. Huang, Phys. Rev. D **64**, 057901 (2001).
- [11] M.A. Ivanov, J.G. Korner, P. Santorelli, Phys. Rev. D **71**, 094006 (2005).
- [12] R. Faustov, V. Galkin, Phys. Rev. D **87**, 034033 (2013).
- [13] S.M. Zhao, X. Liu, S.J. Li, Eur. Phys. J. C **51**, 601 (2007).

Table 2. Branching ratios for the decays above.

	This work	[12]	[17]	[18]	[19]	Experiment [22]
$\bar{B}_s \rightarrow D_s^+ \pi^-$	0.53	0.35	0.5	$0.27^{+0.07}_{-0.03}$	$0.17^{+0.07}_{-0.06}$	0.32 ± 0.4
$\bar{B}_s \rightarrow D_s^+ \rho^-$	1.26	0.94	1.3	$0.64^{+0.17}_{-0.11}$	$0.42^{+1.7}_{-1.4}$	0.74 ± 0.17
$\bar{B}_s \rightarrow D_s^+ K^-$	0.04	0.028	0.04	$0.021^{+0.002}_{-0.002}$	$0.013^{+0.005}_{-0.004}$	
$\bar{B}_s \rightarrow D_s^+ K^{*-}$	0.08	0.047	0.06	$0.038^{+0.005}_{-0.005}$		
$\bar{B}_s \rightarrow D_{s0}^{*+} \pi^-$	0.10	0.09	$0.052^{+0.25}_{-0.021}$			
$\bar{B}_s \rightarrow D_{s0}^{*+} \rho^-$	0.27	0.22	$0.013^{+0.06}_{-0.05}$			
$\bar{B}_s \rightarrow D_{s0}^{*+} K^-$	0.009	0.007	$0.004^{+0.002}_{-0.002}$			
$\bar{B}_s \rightarrow D_{s0}^{*+} K^{*-}$	0.16	0.012	$0.008^{+0.004}_{-0.003}$			
$\bar{B}_s \rightarrow D_s^{*+} \pi^-$	0.45	0.27	0.2	$0.31^{+0.03}_{-0.02}$		0.21 ± 0.06
$\bar{B}_s \rightarrow D_s^{*+} \rho^-$	1.35	0.87	1.3	$0.9^{+1.5}_{-1.5}$		1.03 ± 2.6
$\bar{B}_s \rightarrow D_s^{*+} K^-$	0.04	0.021	0.02	$0.024^{+0.002}_{-0.002}$		
$\bar{B}_s \rightarrow D_s^{*+} K^{*-}$	0.08	0.048	0.06	$0.056^{+0.006}_{-0.007}$		
$\bar{B}_s \rightarrow D_{s1}^+(2460) \pi^-$	0.15	0.19				
$\bar{B}_s \rightarrow D_{s1}^+(2460) \rho^-$	0.36	0.49				
$\bar{B}_s \rightarrow D_{s1}^+(2460) K^-$	0.012	0.014				
$\bar{B}_s \rightarrow D_{s1}^+(2460) K^{*-}$	0.020	0.026				
$\bar{B}_s \rightarrow D_{s1}^+(2536) \pi^-$	0.07	0.029				
$\bar{B}_s \rightarrow D_{s1}^+(2536) \rho^-$	0.19	0.083				
$\bar{B}_s \rightarrow D_{s1}^+(2536) K^-$	0.0054	0.0021				
$\bar{B}_s \rightarrow D_{s1}^+(2536) K^{*-}$	0.01	0.0044				
$\bar{B}_s \rightarrow (2^-)^+ \pi^-$	$7.1 \cdot 10^{-5}$					
$\bar{B}_s \rightarrow (2^-)^+ \rho^-$	0.0047					
$\bar{B}_s \rightarrow (2^-)^+ K^-$	$5.2 \cdot 10^{-6}$					
$\bar{B}_s \rightarrow (2^-)^+ K^{*-}$	$2.2 \cdot 10^{-8}$					
$\bar{B}_s \rightarrow D_{s2}^{*+} \pi^-$	0.1	0.16				
$\bar{B}_s \rightarrow D_{s2}^{*+} \rho^-$	0.27	0.42				
$\bar{B}_s \rightarrow D_{s2}^{*+} K^-$	0.008	0.012				
$\bar{B}_s \rightarrow D_{s2}^{*+} K^{*-}$	0.016	0.022				

- [14] J. Segovia, C. Albertus, D. Entem, F. Fernandez, E. Hernandez et al., Phys. Rev. D **84**, 094029 (2011).
- [15] K. Azizi, Nucl. Phys. B **801**, 70 (2008).
- [16] K. Azizi, M. Bayar, Phys. Rev. D **78**, 054011 (2008).
- [17] P. Blasi, P. Colangelo, G. Nardulli, N. Paver, Phys. Rev. D **49**, 238 (1994).
- [18] X.J. Chen, H.F. Fu, G.L. Wang, J. Phys. G **39**, 045002 (2012)
- [19] R.H. Li, C.D. Lu, Y.M. Wang, Phys. Rev. D **80**, 014005 (2009).
- [20] D. Ebert, R. Faustov, V. Galkin, Phys. Rev. D **75**, 074008 (2007).
- [21] M. Beneke, G. Buchalla, M. Neubert, C.T. Sachrajda, Phys. Rev. Lett. **83**, 1914 (1999).
- [22] J. Beringer *et al.* (Particle Data Group), Phys. Rev. D **86**, 010001 (2012)